AIP | Review of Scientific Instruments

Design and performance of a spin-polarized electron energy loss spectrometer with high momentum resolution

D. Vasilyev and J. Kirschner

Citation: Review of Scientific Instruments **87**, 083902 (2016); doi: 10.1063/1.4961471
View online: http://dx.doi.org/10.1063/1.4961471
View Table of Contents: http://scitation.aip.org/content/aip/journal/rsi/87/8?ver=pdfcov
Published by the AIP Publishing

REVIEW OF SCIENTIFIC INSTRUMENTS **87**, 083902 (2016)

Design and performance of a spin-polarized electron energy loss spectrometer with high momentum resolution

D. Vasilyev and J. Kirschner
Max-Planck-Institut für Mikrostrukturphysik, Weinberg 2, 06120 Halle, Germany

(Received 15 February 2016; accepted 7 August 2016; published online 31 August 2016)

We describe a new "complete" spin-polarized electron energy loss spectrometer comprising a spin-polarized primary electron source, an imaging electron analyzer, and a spin analyzer of the "spin-polarizing mirror" type. Unlike previous instruments, we have a high momentum resolution of less than 0.04 Å^{-1}, at an energy resolution of 90-130 meV. Unlike all previous studies which reported rather broad featureless data in both energy and angle dependence, we find richly structured spectra depending sensitively on small changes of the primary energy, the kinetic energy after scattering, and of the angle of incidence. The key factor is the momentum resolution. *Published by AIP Publishing.* [http://dx.doi.org/10.1063/1.4961471]

I. INTRODUCTION

Spin-polarized electron energy loss spectroscopy (SPEELS) is a powerful tool to study electron excitation dynamics in ferromagnetic and paramagnetic solids. This potential was pointed out in theory,[1–3] and experiment[4,5] in the middle 1980s already. In brief, the experiment requires a spin-polarized electron source,[6] an energy analyzer for the scattered electron, and a spin polarization analyzer. This is called a "complete" experiment and this is what we consider in the following. Several such experiments were built and used successfully.[7–9]

However, with respect to itinerant systems there were some deficiencies found worldwide. They were nicely summarized by Komesu *et al.*[10] in 2006: "In general, these studies report rather broad featureless data in both energy and angle dependence, and this has been attributed to non-conservation of the perpendicular momentum component in the scattering process,[8] nonuniform exchange splitting throughout the Brillouin zone (BZ),[11] and umklapp scattering together with the structure of interband densities of Stoner states in the material."[12]

Several attempts to improve the energy resolution (down to 17 meV[13]) did not substantially remedy this situation and the further development of "complete" SPEELS came to a halt, which lasted for more than 15 years.

In the meantime angle-resolved photoemission in the valence band region was developed to such a state that angular emission features on a scale of 0.035 Å^{-1}[14] or recently down to 0.0049 Å^{-1} were resolved.[15] This suggested that also in SPEELS angular structures on the scale of 0.1 Å^{-1} or less should be observable, provided the scattering geometry on the ingoing and outgoing paths matches this requirement. Indeed, with our new apparatus we detect all the features expected: angular variation on the scale of <0.04 Å^{-1} and sensitivity to the primary energy of less than 0.3 eV. In principle, one should set the primary beam and the take-off angle independently. However, this is technically very difficult. Therefore, we keep the detector angle fixed. The angle 90° is arbitrary, but convenient. The rotation of the target allows to scan the momentum transfer to the target crystal between −2 Å^{-1} and +2 Å^{-1}. We stress that this is now possible because of the now established momentum conservation in the crystal.

For the reader not familiar with SPEELS, we briefly recall the main features of the technique: An electron with well-defined momentum, spin state, and energy is sent onto a ferromagnetic or paramagnetic sample. An electron emitted from the sample (not necessarily the same one) is ejected at a well-defined angle and analyzed with respect to energy and spin orientation relative to the primary one. Neglecting spin-orbit interaction and setting the primary electron spin collinear (not "parallel") with the sample magnetization, we define "up spin" as being aligned along the majority spin direction in the sample (and "down spin" along the polarization of the minority electrons). We send the outgoing electron into a spin analyzer with the spin-sensitive axis along the up-down spin polarization axis. If we detect an "up" electron with the primary electron of "down" type, we may classify this process as "flip down." This configuration corresponds to a Stoner excitation. If we detect a "down" electron this is a non-flip down transition (N_{down} for short). The spin of the detected electrons is the same as that of the primary electron. This may occur in two ways: first, an exchange process within the same spin system, and second a purely dipole transition, i.e., a process where the excitation is independent of the electron spin. These contribute both to the non-flip channels, but their proportion cannot be separated experimentally, only by theory. We will meet these again in Fig. 5 as non-flip resonances.

In the remainder of the paper, we describe the electron-optical components of our new instrument and conclude with some examples of its performance.

II. ELECTRON-OPTICAL COMPONENTS

A. Spin-polarized electron source

Every SPEELS experiment starts with a polarized electron source (Fig. 1). We use photoemission from a strained AlInGaAs/AlGaAs photocathode[16] with emission of 165 nA/1 mW incident light at a wavelength of 826 nm. The intensity is

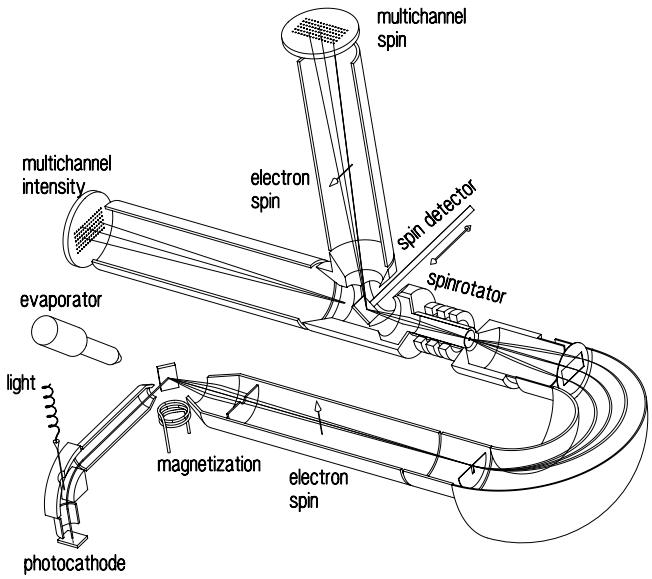

FIG. 1. Schematic drawing of our spin-resolved electron energy loss spectrometer (SPEELS). It consists of a spin-polarized electron source, a transport lens, a hemispherical energy analyzer, a spin-rotator after energy analysis, followed by a spin-polarizing mirror on a retractable holder, and two channel plates with position readout for multichannel operation. The spin-polarizing mirror is shown in the inserted state for multichannel spin detection. When it is in the retracted state, energy loss spectra are obtained in the multichannel mode. The overall energy resolution is 90-130 meV determined by the activation state of the photocathode. The momentum resolution is typically <0.04 Å^{-1}, determined by the apertures in the input lens and the analyzer input. The target can be heated by electron bombardment from the rear (not shown), and the angle of incidence is determined by a rotational feedthrough with vertical rotation axis. Thin films are deposited by the evaporator and are magnetized by short current pulses through the coil ("magnetization").

controlled by a set of wavelength-matched attenuators. In actual measurements, we have to observe two constraints, depending on the mode of measurement. In the intensity asymmetry mode, we have to avoid count rate nonlinearities of the straight through detector. Then we employ emission currents between 0.1 nA and 200 nA. For polarization asymmetry measurements we could turn up the light intensity strongly, but we observed that the spin polarization drops. This is caused by heating of the cathode (we observed cathode temperatures up to 80 °C). Therefore, in this mode we use 0.4 to 1 μA emission current.

The photocathode is cleaned by atomic hydrogen[17] at 520 °C for 30 min, followed by a short anneal at 550 °C for 10 min. The cathode is activated by the standard yo-yo procedure with O_2 and Cs. The useful lifetime of the photocathode is of the order several months, with some intermediate reactivation with Cs and O_2 if needed.

The photoelectrons are extracted by a multi-element aperture lens system and focused into a spherical deflector (deflection angle 90°), with entrance and exit apertures of 1 mm diameter each. It is not used as a dispersing element because the loss of intensity would be too severe. After the exit aperture, the beam is converged to a nearly parallel beam by a 5-element asymmetrical electrostatic zoom lens onto the target. The beam diameter of 1–1.2 FWHM mm was determined by scanning a sharp edge of the sample across the beam and measuring the scattered intensity. The source is nearly identical to the one described in Ref. 18. The energy range used here is 10–50 eV. The overall angular resolution was determined to be $\Delta K = 0.045$ Å^{-1}. For the energy resolution of the primary beam, we quote a range of 90–130 meV FWMH. For a freshly prepared cathode we find 130 meV (high photocurrent). For an aged cathode we find 90 meV (reduced current). The crucial parameter is the position of the vacuum level relative to the bottom of the conduction band. The majority of photoelectrons do not escape into vacuum from the bottom of the conduction band but from the band-bending region (BBR). For the electrons thermalized to the BBR, depolarization can be observed because they have a higher probability to depolarize because of their longer escaping time. Therefore the position of the vacuum level controls the energy resolution and the spin-polarization of the beam.

B. Sample preparation

We use epitaxial films of, e.g., Fe or Co in the monolayer thickness range grown epitaxially on Ir(100). Ir can easily be cleaned by cyclic heating in oxygen along the procedures given in Ref. 19. Fe and Co both grow in a (1×1) structure, without intermixing. The composition of the films (or sandwiches) is checked by an Auger analyzer of cylindrical mirror analyzer (CMA) type, incorporated into the system.

A qualitative structure check may be obtained by rotating the sample under the primary beam and observing the elastically diffracted electrons when the beams sweep across the main analyzer entrance. This gives information about the existence of higher order beams and their approximate profiles. A further check on the thickness of the Fe layer is provided by its peculiar magnetic behavior: below about 5 ML clean films behave paramagnetic, above that they are ferromagnetic. This discontinuity can be used to calibrate the electron beam evaporator.[20,21] The films are magnetized by short current pulses created by discharging a capacitor bank ("magnetization" in Fig. 1). The samples are measured in remanence. For films in the monolayer range, the stray field should be negligible and no such effects have been observed.

C. Energy- and momentum-analysis

The electrons leaving the target with or without energy loss are collected by the entrance lens of the spectrometer (Phoibos 150 WAL, manufactured by SPECS[22]). The opening angle is determined by an iris aperture and by the entrance aperture to the hemispherical analyzer. Their trajectories are dispersed inside the hemisphere and re-focused after the rectangular exit aperture into the entrance of the spin rotator. For intensity measurements, the polarizing mirror (shown inserted) is retracted and the electron source is imaged onto a double channel plate detector. Because we do not monochromatize the primary beam, the overall energy resolution is determined ultimately by the primary beam energy width. This in turn depends on the work function of the photocathode.

While the energy resolution is of great importance, we found that the momentum resolution is of even higher importance for SPEELS. Our sample manipulator is equipped with a motor-driven rotary drive with a resolution of 0.005°. We take rotation profiles which are of rectangular shape for the

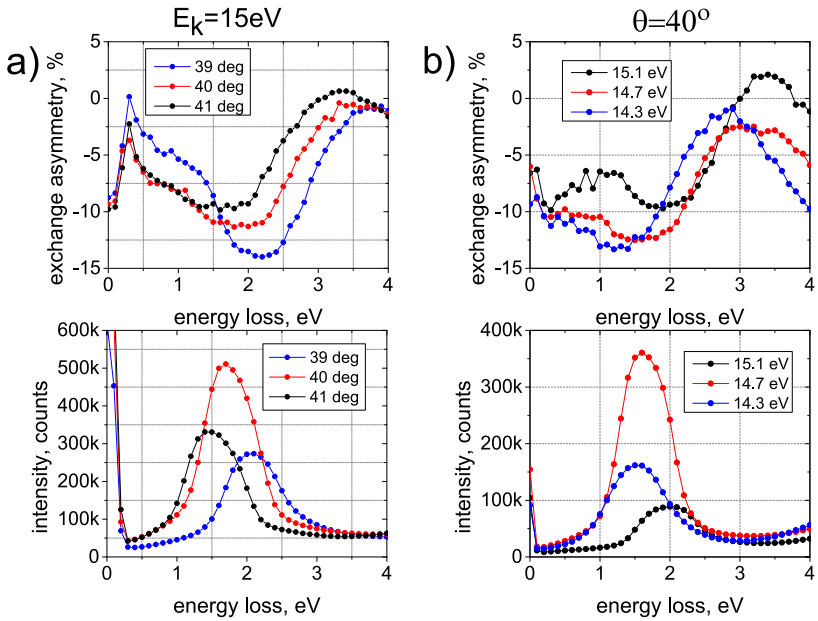

FIG. 2. Electron energy loss spectra from 6 ML Fe on Ir(100) for constant primary energy when varying the angle of incidence (Fig. 2(a), primary energy 15 eV) or at constant angle for varying the primary energy by ±0.4 eV (Fig. 2(b), angle 40°). These data prove the pronounced sensitivity of SPEELS with respect to small changes of angle and primary energy.

specular beam around $\Theta = 45°$. The edges of the profile show a resolution of 0.01° (not the width of the profiles but of their edges). This translates into a momentum resolution of $\Delta K_{||} \leq 0.045$ Å^{-1}. Hence, if the wavevector is conserved during scattering we would expect strong intensity variations if, for constant energy, we change the scattering angle by the order of 1°. Conversely, at constant scattering angle, we may expect sizeable structures if we change the primary energy

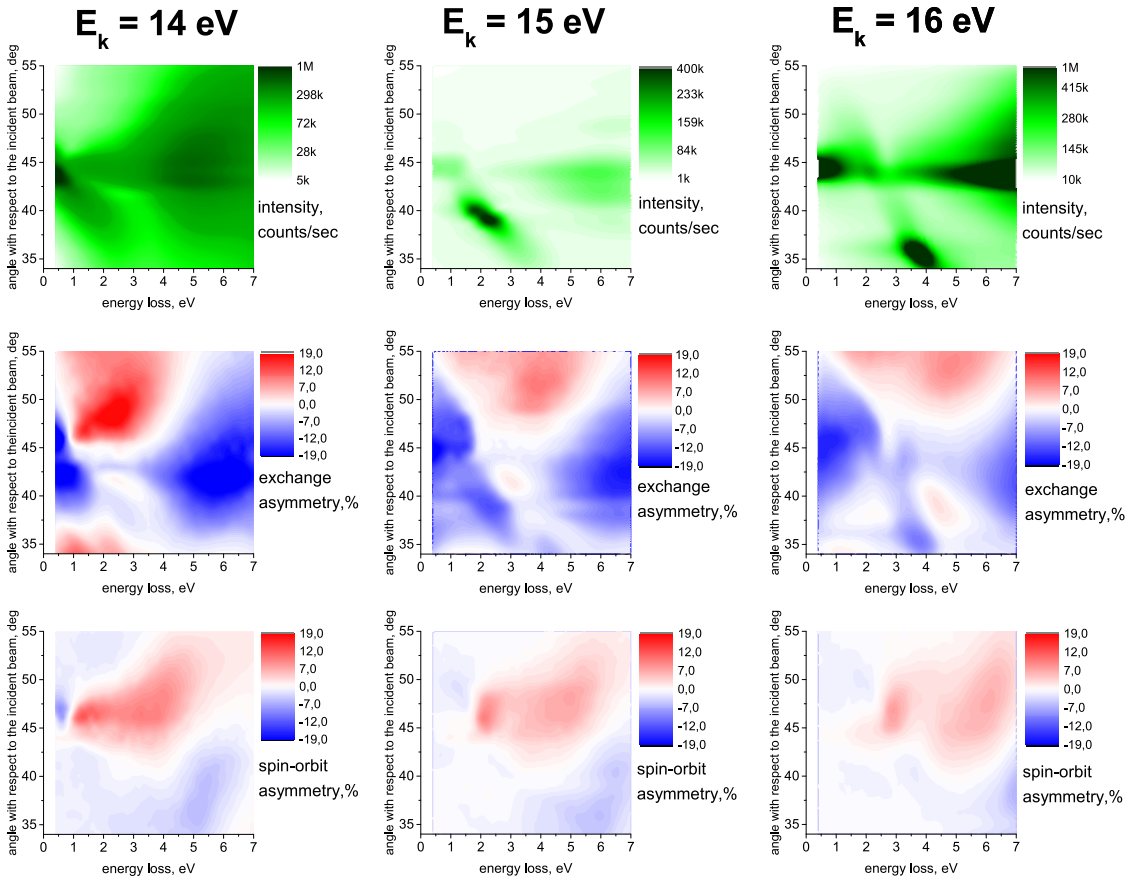

FIG. 3. Results for intensity (top row), exchange asymmetry (center row), and spin-orbit asymmetry (bottom row) from 6 ML Fe on Ir(100) for three primary energies. In each panel, the horizontal axis is the energy loss. The vertical scale shows the angle of incidence of the primary beam. Note the richness of structures and the sensitivity with respect to small changes of primary energy, loss energy, and angle of incidence.

by 1 eV or less. This is indeed the case as demonstrated by Fig. 2. The structures are essentially due to non-flip transitions as demonstrated below.

In Fig. 3, we display the intensity (top row), the exchange asymmetry in the center row, and the spin-orbit asymmetry (bottom row) for primary energies of 14, 15, and 16 eV in the form of color-coded landscapes. The distributions are strongly structured. They may serve as a benchmark for future SPEELS calculations.

D. Spin-polarization analysis

After energy analysis, the beam is focused into the spin rotator. An ideal spin rotator consists of a homogeneous magnetic field oriented parallel to the trajectory of an incident electron beam. It acts on the spin orthogonal to its trajectory and rotates the spin in a plane orthogonal to the field direction by an amount proportional to the field strength. The direction is clockwise or anti-clockwise depending on the spin orientation and the field direction. In principle, there is no influence on the angular spread of the beam. The purpose is to align the electron spin after the energy analyzer with the spin-sensitive axis of the spin-sensitive electron mirror which is the normal to the scattering plane (due to spin-orbit interaction). In operation, we compare the count rate with the spin configuration shown with that when all spin arrows are reversed. The asymmetry of the count rates can be more than 50% (see e.g., Fig. 5). For a rotation of the spin by 90° a current of about 100 mA is required.

The operating principle of our spin analysis is that of the "spin polarizing mirror." It relies on the conservation of the parallel momentum of the specular LEED beam upon reflection from a single crystal surface, independent of the energy of the elastically scattered electron. In the same way as one does for a multichannel intensity detector one may also build a multichannel spin detector. This mode of operation is obtained by inserting the detector crystal into the outgoing beam after the spin rotator (see Fig. 1) and using a second multichannel plate at 90° from the straight-through beam.

The heart of the spin detector is a pseudomorphic monolayer of Au on Ir(100). It is prepared by depositing several monolayers of Au, followed by a series of flashes to a temperature slightly below the desorption temperature of the monolayer. This has been described in Ref. 23.

A further point to be mentioned is the time stability of the detector crystal. As long as the vacuum remains in the range of $\leq 10^{-10}$ mbar, the detector sensitivity remains stable. Only after venting the system, a new pseudomorphic Au-layer needs to be prepared. The lifetime of the detector is virtually infinite. We claim more than 10 months since so far this is the maximum time between two ventings of the system.

III. EXAMPLES

A. Stoner excitations

The examples for the study of the exchange and spin-orbit asymmetries given above make no explicit use of the electron spin polarization of the scattered electrons and therefore demonstrate only half of the capabilities of our new instrument. If, for example, the primary electron is in the "up" state and the scattered electron is in the "down" state, we term this a "flip" event (F_{up}). Conversely, if the scattered electron is found in the "up" state we term this a non-flip (N_{up}) event. A full measurement at a given energy involves four measurements, two for each spin state of the primary electron, and two for each magnetization direction of the target. In addition, we measure two total intensities giving rise to an exchange asymmetry A_{ex}, neglecting the spin-orbit asymmetry A_{so}. From these four measurements, one may derive four partial intensities (F_{up}, F_{down}, N_{up}, N_{down}) along the lines given in Ref. 5. When normalized to the sum of the count rates, we obtain the percentage of each of the four transition processes. See Fig. 4.

Of particular interest among those is the channel F_{down}, since the electron configuration in the excited state corresponds to a Stoner excitation: We send in a primary electron of minority character which finds a place in an empty minority band above the Fermi energy. The kinetic energy released in this transition is used to release a majority electron from below E_F which is detected outside of the target, leaving a hole. Thus, we have created an electron-hole pair of Stoner character. Its energy is reflected in the energy loss, which peaks around 2 eV and dominates all other normalized transition probabilities (blue line). At zero energy loss, we find no such excitation probability, as well as for the reverse Stoner excitation (red line). The momentum of the Stoner pair corresponds to the difference of the momenta of the primary electron and the

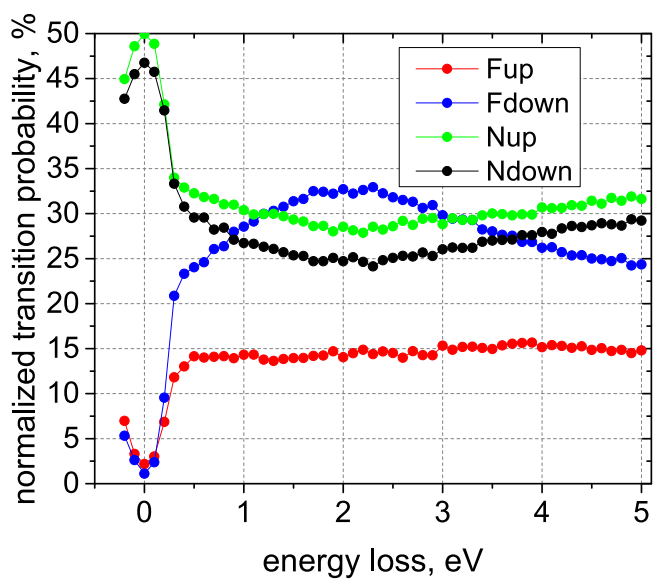

FIG. 4. A typical result of a SPEELS measurement on an itinerant ferromagnet. The sum of the partial transition probabilities is normalized to 100%. At zero energy loss, i.e., for strictly elastic scattering, the flip intensities F_{up} and F_{down} are zero within statistics because flip processes with non-zero probabilities do not exist. The non-flip processes are strong and reach almost 50% each. The small but significant difference between N_{up} and N_{down} gives rise to the elastic exchange asymmetry, known from spin polarized LEED. Parameters are 6 ML Fe on Ir(100), primary energy 16 eV, angle of incidence $\Theta = 60°$ with respect to the surface normal, and momentum transfer $\Delta K_{||} = -0.75$ Å^{-1} along $\Gamma - X$. The F-channels indicate the creation of electron-hole pairs with opposite spin (Stoner pairs indicated by the blue line (F_{down})). The N-channels represent non-flip transitions (i.e., without spin reversal), black and green.

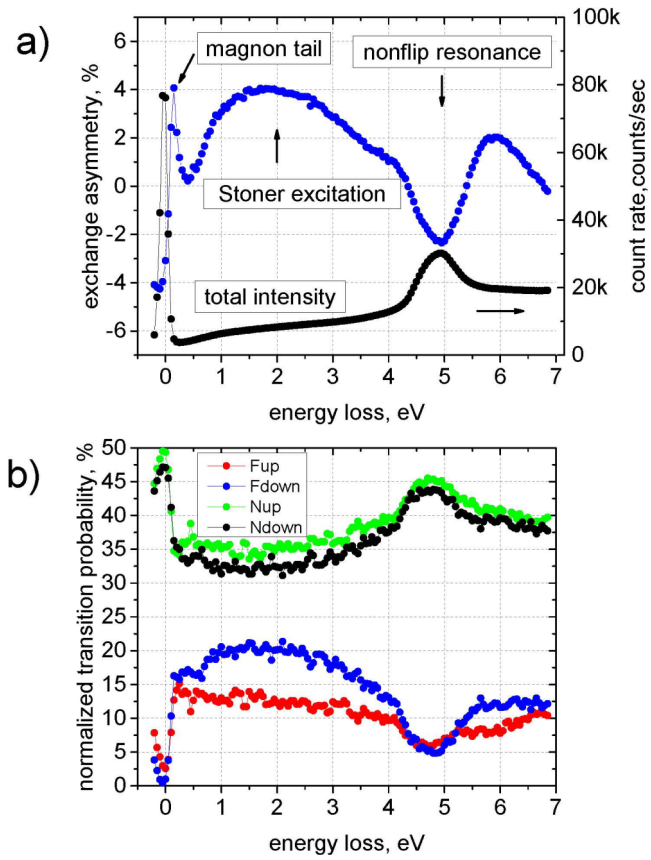

FIG. 5. This figure shows a compilation of all excitation processes that may be observed by SPEELS. The black curve shows the total intensity scale on the right hand side. Next to the elastic peak we observe a second narrow peak, displaced by a few tenths of an eV, which we label "magnon tail." The asymmetry starts at 4%, rises rapidly, and falls off towards higher energy loss. This comes about by the quasielastic peak masking the low energy part by electrons of small asymmetry (blue curve). For the direction towards higher energy loss we find an extended region of Stoner excitations and, as the red curve shows, of inverted Stoner excitations of F_{up} type. At about 5 eV energy loss, we find a peak in the intensity, a peak in the nonflip asymmetry in Fig. 5(b) (green and black), and a minimum in the flip asymmetry F_{up} and F_{down}. These structures are caused by the non-flip transition and we call the structure "nonflip resonance." They are of the same nature as in Fig. 2, bottom panels.

detected electron, as given by the geometry and the energy. The non-flip transitions at zero energy loss indicate the scattered electron having the same spin character as the primary electron. This indicated dipolar scattering or an exchange process within the same spin system. This cannot be distinguished experimentally but needs theoretical calculations. The difference between green and black intensities at zero energy loss corresponds to the elastic exchange asymmetry.

B. Coexistence of collective and single particle excitations

In metallic ferromagnets, two types of elementary magnetic excitations can exist: collective excitations, called magnons, and single particle electron-hole pairs, called Stoner excitations. The relative abundances are not known, neither experimentally nor theoretically, since a quantitative theory of SPEELS does not exist yet. With our new SPEELS system we can see them both, though the magnons are partially masked by quasielastically scattered primaries. In Fig. 5 we identify the Stoner excitations, the "magnon tail," and a third contribution of dipolar character which we call "non-flip resonance." At the quasielastic peak (zero energy loss in Fig. 5(a)), the exchange asymmetry happens to be negative for our choice of parameters. The magnons contribution is very small at or slightly above zero energy loss, so that the exchange asymmetry is negative at −4%. Going to non-zero but small energy loss, the elastically scattered primaries die out and the total asymmetry becomes positive (+4%) because of angular momentum conservation in magnon excitation. This sign is the same for Stoner excitations near 2 eV loss energy (blue curve in Fig. 5(a)). Between 4 and 5 eV loss energy we find a further change of signs in the exchange asymmetry, a relative peak in the non-flip channels N_{up} and N_{down}, a minimum in the flip channels F_{up} and F_{down}, and a relative maximum in the total count rate (see Fig. 5(b)). More than 90% of the total count rate is due to the non-flip channels N_{up} and N_{down}. Therefore we call this feature tentatively a "non-flip resonance."

IV. CONCLUSIONS

Our new instrument for spin-polarized electron energy loss spectroscopy (SPEELS) seems to be a rather versatile and powerful device to study elementary excitations in ferromagnets and paramagnets. We may observe exchange and dipolar scattering processes and we may observe magnon excitations and electron hole pairs (Stoner excitations) in great detail. The key to these features is the greatly improved momentum resolution compared to the previous instruments.

ACKNOWLEDGMENTS

The present prototype instrument was developed in collaboration with the SPECS company, Berlin. Special thanks are due to O. Schaff, Th. Kampen, D. Funnemann, and B. Johansson. Technical support by H. Engelhard, D. Hartung, H. Menge, and T. Braun is gratefully acknowledged.

[1]J. Glazer and E. Tosatti, "Theory of spin-flip excitations across the ferromagnetic Stoner gap in electron energy loss," Solid State Commun. **52**, 905 (1984).
[2]C. J. Bocchetta, E. Tosatti, and S. Yin, "Spin flip inelastic scattering in electron energy loss spectroscopy of a ferromagnetic metal," Z. Phys. B: Condens. Matter **67**, 89 (1987).
[3]G. Vignale and K. S. Singwi, "Spin-flip electron-energy-loss spectroscopy in itinerant-electron ferromagnets: Collective modes versus Stoner excitations," Phys. Rev. B **32**, 2824 (1985).
[4]J. Kirschner, "Direct and exchange contributions in inelastic scattering of spin-polarized electrons from iron," Phys. Rev. Lett. **55**, 973 (1985).
[5]D. Venus and J. Kirschner, "Momentum dependence of the Stoner excitation spectrum of iron using spin-polarized electron-energy-loss spectroscopy," Phys. Rev. B **37**, 2199 (1988).
[6]G. Lampel and C. Weisbuch, "Proposal for an efficient source of polarized photoelectrons from semiconductors," Solid State Commun. **16**, 877 (1975); D. T. Pierce, F. Meier, and P. Zürcher, "Negative electron affinity GaAs: A new source of spin-polarized electrons," Appl. Phys. Lett. **26**, 670 (1975); D. T. Pierce, R. J. Celotta, G.-C. Wang, W. N. Unertl, A. Galejs, C. E. Kuyatt, and S. R. Mielczarek, "GaAs spin polarized electron source," Rev. Sci. Instrum. **51**, 478 (1980); T. Omori, Y. Kurihara, T. Nakanishi, H. Aoyagi, T. Baba, T. Furuya, K. Itoga, M. Mizuta, S. Nakamura, Y. Takeuchi,

M. Tsubata, and M. Yoshioka, "Large enhancement of polarization observed by extracted electrons from the AlGaAs-GaAs superlattice," Phys. Rev. Lett. **67**, 3294 (1991); T. Maruyama, E. L. Garwin, R. Prepost, G. H. Zapalac, J. S. Smith, and J. D. Walker, "Observation of strain-enhanced electron-spin polarization in photoemission from InGaAs," *ibid.* **66**, 2376 (1991); T. Nakanashi, H. Aoyagi, H. Horinaka, Y. Kamiya, T. Kato, S. Nakamura, T. Saka, and M. Tsubata, "Large enhancement of spin polarization observed by photoelectrons from a strained GaAs layer," Phys. Lett. A **158**, 345 (1991); T. Omori, Y. Kurihara, Y. Takeuchi, M. Yoshioka, T. Nakanashi, S. Okumi, M. Tsubata, M. Tawada, K. Togawa, Y. Tanimoto, C. Takahashi, T. Baba, and M. Mizuta, "Highly polarized electron source using InGaAs-GaAs strained-layer superlattice," Jpn. J. Appl. Phys., Part 1 **33**, 5676 (1994).

[7]G. A. Mulhollan, X. Zhang, F. B. Dunning, and G. K. Walters, "Inelastic spin-exchange scattering of electrons from paramagnetic metals," Phys. Rev. B **41**, 8122 (1990).

[8]K.-P. Kämper, D. L. Abraham, and H. Hopster, "Spin-polarized electron-energy-loss spectroscopy on epitaxial fcc Co layers on Cu(001)," Phys. Rev. B **45**, 14335 (1992).

[9]B. Fromme, M. Schmitt, E. Kisker, A. Gorschlüter, and H. Merz, "Spin-flip low-energy electron-exchange scattering in NiO(100)," Phys. Rev. B **50**, 1874 (1994).

[10]T. Komesu, G. D. Waddill, and J. G. Tobin, "Spin-polarized electron energy loss spectroscopy on Fe(100) thin films grown on Ag(100)," J. Phys.: Condens. Matter **18**, 8829 (2006).

[11]J. Kirschner, D. Rebenstorff, and H. Ibach, "High-resolution spin-polarized electron-energy-loss-spectroscopy and the Stoner excitation spectrum in nickel," Phys. Rev. Lett. **53**, 698 (1984).

[12]R. Saniz and S. P. Apell, "Interpretation of spin-polarized electron energy loss spectra," Phys. Rev. B **63**, 014409 (2000).

[13]D. L. Abraham and H. Hopster, "Spin-polarized electron-energy-loss spectroscopy on Ni," Phys. Rev. Lett. **62**, 1157 (1989).

[14]A. Winkelmann, M. Ellguth, C. Tusche, A. A. Ünal, J. Henk, and J. Kirschner, "Momentum-resolved photoelectron interference in crystal surface barrier scattering," Phys. Rev. B **86**, 085427 (2012).

[15]C. Tusche, A. Krasyuk, and J. Kirschner, "Spin resolved band structure imaging with a high resolution momentum microscope," Ultramicroscopy **159**, 520 (2015).

[16]Y. A. Mamaev, L. G. Gerchikov, Y. P. Yashin, D. A. Vasilyev, V. V. Kuzmichev, V. M. Ustinov, A. E. Zhukov, V. S. Mikhron, and A. P. Vasiliev, "Optimized photocathode for spin-polarized electron sources," Appl. Phys. Lett. **93**, 081114 (2008).

[17]Atomic hydrogen source EFM-H, Focus GmbH, 2016, www.focus-gmbh.com.

[18]A. V. Pradeep, A. Roy, P. S. Anil Kumar, and J. Kirschner, "Development of a spin polarized low energy electron diffraction system," Rev. Sci. Instrum. **87**, 023906 (2016).

[19]Kh. Zakeri, T. R. F. Peixoto, Y. Zhang, J. Prokop, and J. Kirschner, "On the preparation of clean tungsten single crystals," Surf. Sci. **604**, L1–L3 (2010).

[20]J. Kirschner, H. Engelhard, and D. Hartung, "An evaporation source for ion beam assisted deposition in ultrahigh vacuum," Rev. Sci. Instrum. **73**, 3853 (2002).

[21]T.-H. Chuang, Kh. Zakeri, A. Ernst, Y. Zhang, H. J. Qin, Y. Meng, Y.-J. Chen, and J. Kirschner, "Magnetic properties and magnon excitations in Fe(001) films grown on Ir(001)," Phys. Rev. B **89**, 174404 (2014).

[22]PHOIBOS 150 WAL, SPECS, 2016, www.specs.de.

[23]D. Vasilyev, C. Tusche, F. Giebels, H. Gollisch, R. Feder, and J. Kirschner, "Low-energy electron reflection from Au-passivated Ir(001) for application in imaging spin-filters," J. Electron Spectrosc. Relat. Phenom. **199**, 10 (2015).